EEG topographic features for assessing skill levels during laparoscopic surgical training

Takahiro Manabe, Pushpinder Walia, Yaoyu Fu, Steven Schwaitzberg, Lora Cavuoto, Anirban Dutta
University at Buffalo
Buffalo, NY
loracavu@buffalo.edu, anirband@buffalo.edu

Xavier Intes, Suvranu De
Rensselaer Polytechnic Institute
Troy, NY
INTESX@rpi.edu, des@rpi.edu

ABSTRACT

Objective: The objective of this study was to evaluate the differences in brain activity between expert surgeons and novice medical residents based on electroencephalography (EEG). The first sub-goal was to assess the Microstate EEGlab toolbox and BCIlab toolboxes for data analysis and classification of the topographical features for microstate-based Common Spatial Pattern (CSP) analysis. Then, the second sub-goal was to compare microstate-based CSP with the conventional regularized CSP approach.
Methods: After IRB approval, ten expert surgeons and 13 novice medical residents were recruited at the University at Buffalo. After informed consent, the subjects performed three trials of laparoscopic suturing and knot tying with rest periods in-between the task trials. 32-channel EEG was performed during the task performance that was used to analyze spatial patterns of brain activity in 8 expert surgeons (2 dropouts due to data quality) and 13 novice medical residents. Microstate analysis was applied as preprocessing to improve the signal-to-noise ratio before CSP analysis, distinguishing expert surgeons' brain activity from novice medical residents.
Results: Microstate-based CSP analysis identified the significant channels based on the maximum spatial pattern vectors at the scalp. While novices had primarily the frontal cortex involved for a maximum of the spatial pattern vectors at the scalp, the experts had the hotspot of the spatial pattern vectors over the frontal and parietal cortices. Simple linear discriminant analysis with 10-fold cross-validation achieved more than 90% classification accuracy with microstate-based CSP, while the conventional regularized CSP could reach around 80% classification accuracy.
Conclusion and Discussion: Microstate-based CSP analysis can identify an optimal set of channels for evaluating the differences in brain activity between expert surgeons and novice medical residents. Future studies can apply microstate-based monitoring of the temporal dynamics of the brain behavior for an individualized adaptive VR-based training paradigm.

ABOUT THE AUTHORS

Takahiro Manabe is an undergraduate exchange student at the University at Buffalo.

Pushpinder Walia is a graduate student at the University at Buffalo.

Yaoyu Fu is a post-doctoral fellow at the University at Buffalo.

Xavier Intes is a faculty at the Rensselaer Polytechnic Institute.

Steven Schwaitzberg is a faculty at the University at Buffalo.

Suvranu De is a faculty at the Rensselaer Polytechnic Institute.

Lora Cavuoto is a faculty at the University at Buffalo.

Anirban Dutta is a faculty at the University at Buffalo.

EEG features for assessing skill levels during laparoscopic surgical training

Takahiro Manabe, Pushpinder Walia, Yaoyu Fu, Steven Schwaitzberg, Lora Cavuoto, Anirban Dutta
University at Buffalo
Buffalo, NY
loracavu@buffalo.edu, anirband@buffalo.edu

Xavier Intes, Suvranu De
Rensselaer Polytechnic Institute
Troy, NY
INTESX@rpi.edu, des@rpi.edu

Introduction

Laparoscopic surgery training following the Fundamentals of Laparoscopic Surgery (FLS) curriculum is a common education and training module designed for medical residents, fellows, and physicians to assess a set of basic surgical skills necessary to conduct laparoscopic surgery successfully. The FLS training is a joint program between the Society of American Gastrointestinal and Endoscopic Surgeons and the American College of Surgeons required to receive board certification in general surgery in the US (Birkmeyer et al., 2013). FLS certification uses five psychomotor tasks with increasing task complexity: (i) pegboard transfers, (ii) pattern cutting, (iii) placement of a ligating loop, (iv) suturing with extracorporeal knot tying, and (v) suturing with intracorporal knot tying. It was introduced to systemize training and evaluation of cognitive and psychomotor skills required to perform minimally invasive surgery. The FLS curriculum is being used to measure and document those skills for medical practitioners. Here, understanding the brain-behavior relationship is crucial for informed training and assessment (Dehabadi et al., 2014), especially for assessing skill levels.

In the context of skill assessment under perception-action coupling theory (Voorhorst et al., 1998), the novice brain is postulated to build a cognitive-perceptual mental model (Cioffi, 1991; Renner et al., 2013) under perceptual load (Marucci et al., 2021) at the start of FLS skill acquisition (Kamat et al., 2022; Riener & Harders, 2012). Here, the central nervous system internally simulates the motor behavior in planning, control, and learning such that the prediction of the sensory input is compared with the reafferent sensory information to determine the discrepancy that is postulated under the forward model concept (Wolpert & Miall, 1996),(Kawato, 1999),(Kamat et al., 2022). Then, deliberate practice (Ericsson & Harwell, 2019) can reduce the discrepancy by actively probing the environment which can lead to expert performance. Here, action-to-perception coupling for actively probing the environment is not only crucial for motor skill training (Riener & Harders, 2012) but also for discriminating movement-related sensations from environmental stimuli (Sommer & Wurtz, 2008). Christensen et al. (Christensen et al., 2014) investigated the action-perception coupling based on the effect of action execution on action perception. Here, exploratory action for perception (Hurley, 2001), which facilitates the closure of the perception-action cycle, is postulated in novices during skill acquisition. In this study, we postulate that the EEG features of the perception-action cycle can be used to discriminate experts from novices during FLS suturing with intracorporal knot tying.

Computational circuit mechanisms (Gu et al., 2021) have presented selective attention (Crick, 1984) or excitability with the thalamus (Hughes et al., 2004) acting as a "spotlight" that is postulated to be a microstate in the brain – defined as a short epoch – during which the scalp potential field from electroencephalogram (EEG) remains semi-stable (Michel & Koenig, 2018). This "spotlight" approach leads to a crucial a priori assumption that only one spatial map entirely defines the relevant global state of the brain at each moment in time, and the residuals are considered noise (Michel & Koenig, 2018). Here, the temporal evolution of the spatial map in novices is postulated to differ from experts who have well-developed cognitive-perceptual models and may have achieved particular motor skill "automaticity" (Poldrack et al., 2005). Specifically, spatiotemporal patterns of neural activity for selection in working memory and perception in experts will differ from novices (Tamber-Rosenau et al., 2011) that can be captured with the scalp potential field from EEG.

In this study, we used microstate analysis to leverage the excellent temporal resolution of EEG (Michel & Koenig, 2018) for detecting the semi-stable scalp potential field at the start of the FLS suturing with intracorporeal knot tying task (henceforth, the FLS task). Then, we applied Common Spatial Pattern (CSP) for feature extraction, where the algorithm finds spatial filters (Koles, 1991) for two classes of data – experts and novices. The traditional

CSP method suffers from noise sensitivity due to the L2 norm in its optimization problem. Our microstate-based CSP approach addressed this with a meta-criterion favoring the highest signal-to-noise ratio (Custo et al., 2017).

Methods

Subjects and Experimental Setup

After written consent, 13 healthy novice medical students and ten expert surgeons were recruited to perform the FLS task. The study was approved by the Institutional Review Board of the University at Buffalo, NY. All study procedures were performed according to local research regulations for human subjects. The experts had substantial experience with laparoscopic suturing, whereas the novices were entirely new to the task. All the subjects were instructed verbally with a standard set of instructions on how to complete the suturing with intracorporeal knot tying task to the best of their capacity. Participants were provided with two laparoscopic needle drivers, one suturing scissors, and a needle with a suture of 15 cm in length. The task involves inserting the suture through two marks in a Penrose drain and then tying a double-throw knot followed by two single-throw knots using two needle drivers operated by both hands. The task starts when the subject picks up the suture and needle driver on the start command and ends when the subject cuts both ends of the suture.

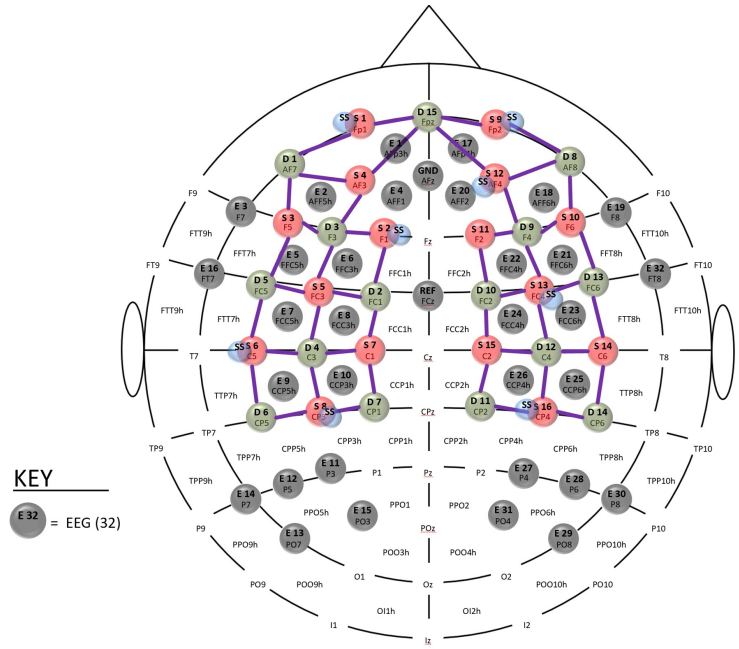

(A)

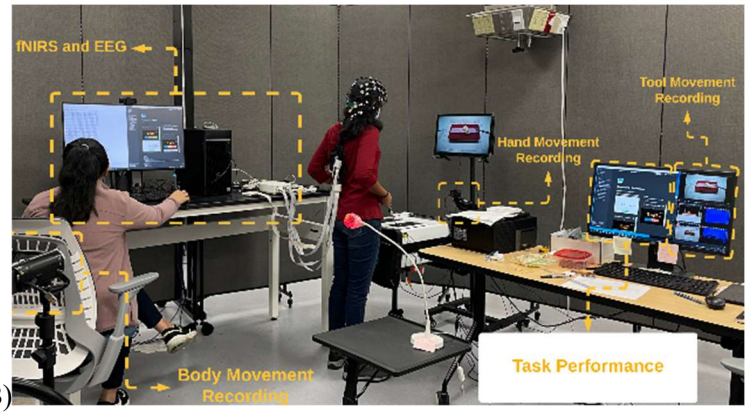

(B)

(C) 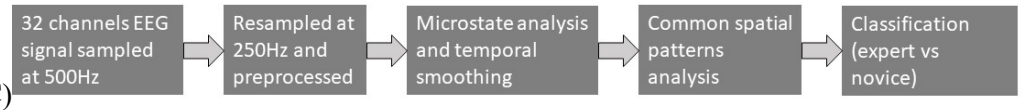

Figure 1: (A) Sensor montage with active gel-electrodes shown with 'E' grey discs. (B) Experimental setup. (C) EEG data processing pipeline in EEGLab and BCILab for the classification of expert vs. novice.

A customized montage consisting of EEG sensors was used to record brain activation signals. Thirty-two channels of EEG signals were recorded using a wireless LiveAmp system (Brain Vision, USA). EEG recordings were obtained at 500 Hz using active gel electrodes, as shown with 'E' grey discs in Figure 1A. Figure 1B shows the experimental brain-behavior setup in the laboratory.

Data processing in EEGLab and BCILab

The recorded EEG was preprocessed and analyzed offline using the open-source EEGLab toolbox (https://sccn.ucsd.edu/eeglab/index.php) for the microstate analysis (Michel & Koenig, 2018). Specifically, the data were downsampled to 250Hz and high-pass filtered at 1Hz. Then, the line noise was removed using the 'cleanline' function, followed by the 'clean_rawdata' function to reject bad channels. The bad channels were interpolated using spherical splines (Perrin et al., 1989) in 'clean_rawdata' followed by re-referencing to the global average. The task epochs were defined manually as ±10sec around the task trigger postulated to be the start of building a cognitive-perceptual model (Cioffi, 1991; Renner et al., 2013). Then, artifact subspace reconstruction (ASR) was performed using the default settings in EEGLab, followed by re-referencing to the global average. ASR was performed using the default settings in EEGlab, followed by re-referencing to the global average. Then, Laplacian spatial filter was applied to remove the volume conduction from subcortical sources since we were interested in the cortical sources. Here, ASR is an automated method based on a user-specified parameter that can effectively remove transient EEG artifacts (Chang et al., 2020). We used the default ASR parameter value of 20, and the optimal value is between 20 and 30 to balance between removing non-brain signals and retaining brain activities (Chang et al., 2020). In this study on the EEG topographic features, the maximum number of bad channels allowed for any subject was less than five, so we dropped two expert subjects.

Microstate analysis was performed using the EEGlab toolbox (Poulsen et al., 2018) after aggregating EEG data during the FLS task from all the experts (N=8) and novices (N=13). First, we identified EEG microstate prototypes based on modified K-means clustering in the EEGlab. The modified K-means clustering was based on the goodness of fit of the microstate segmentation determined from the global explained variance (GEV) and the cross-validation criterion (CV). Here, the GEV criterion should theoretically become monotonically larger with the increasing number of clusters (Poulsen et al., 2018). The modified K-means clustering in EEGlab finds topographical maps of polarity invariant microstate prototypes (Poulsen et al., 2018) from the spontaneous EEG data during the FLS task (and rest periods in between the trials). Here, global field power (GFP) peaks are used to segment the EEG time series. The minimum peak distance was set at 10ms (default), and 1000 randomly selected peaks (default) per subject were used for the segmentation. Then, we rejected the GFP peaks that exceeded one time the standard deviation of all the GFPs of all maps to segment the EEG data into a predefined number (2 to 8) of microstates. Here, the goal is to maximize the similarity between the EEG samples and the prototypes of the microstates they are assigned to using the modified K-means algorithm (Poulsen et al., 2018). The modified K-means algorithm also sorts the microstate prototypes in decreasing GEV. We had set 100 random number of initializations and 1000 maximum iterations for the modified K-means algorithm with the 1e-6 (default) as the relative threshold of convergence (Poulsen et al., 2018). These microstates provided the prototypes for the subsequent microstate-based CSP analysis.

Microstate labels were applied to the EEG samples from the experts and novices based on topographical similarity (called backfitting) using the EEGlab toolbox (Poulsen et al., 2018). Since short periods of unstable EEG topographies can occur, so, we applied temporal smoothing. Then, the temporally smoothed EEG topographies from the experts (N=8) and novices (N=13) at the start of the FLS task in a 10-sec epoch were subjected to CSP analysis and classification using the BCILab (Kothe & Makeig, 2013). Here, if X_1 and X_2 are the EEG topographies from the experts and novices at the start of the FLS task, viz., X_i is a matrix of rows 250Hz times 10sec and columns 32 channels, then the desired spatial filter is obtained by, $\underset{w}{\operatorname{argmax}} J(w) = \frac{w^T X_1^T X_1 w}{w^T X_2^T X_2 w} = \frac{w^T C_1 w}{w^T C_2 w}$, where w denotes the spatial filter and C_1 and C_2 represent the covariance matrices of X_1 and X_2 respectively. Using the Lagrange multiplier approach, the

optimization problem can be written as, $L(\lambda, w) = w^T C_1 w - \lambda(w^T C_2 w)$, where λ is the Lagrange multiplier. The optimization problem to find the spatial filter, *w*, requires the derivative set to zero, i.e., $\frac{\delta L}{\delta w} = 2w^T C_1 - 2\lambda w^T C_2 = 0$. The solution of this optimization problem are the eigenvectors, $M = C_2^{-1} C_1$, representing the spatial pattern vectors at the scalp. Here, the regularized CSP can improve the robustness in small sample setting (Lu et al., 2010), and the largest eigenvector from, $M_1 = (C_2 + \alpha K)^{-1} C_1$, and $M_2 = (C_1 + \alpha K)^{-1} C_2$, represent the spatial pattern vectors at the scalp with K assumed as an identity matrix (Lotte & Guan, 2011). Then, the classification was performed using simple linear discriminant analysis (LDA) with 10-fold cross-validation. The computational pipeline, starting from the raw EEG data to the classification, is shown in Figure 1C.

Results

We selected six EEG microstate prototypes based on the GEV and the CV criterion, as shown in Figure 2A. Here, the CV criterion, pointing to the best clustering solution at its smallest value, reached the minimum value for six microstates that are shown in Figure 2B, sorted in decreasing GEV. As expected for a visuomotor task, the highest GEV is for the microstate 1, corresponding to the activation of the visual cortex (visual imagery (Britz et al., 2010)). The six microstate prototypes were backfitted to the EEG for 10 sec at the start of the FLS task (postulated to be the start of building a cognitive-perceptual model (Cioffi, 1991; Renner et al., 2013) in novices), as shown in Figure 3, for an illustrative novice (Figure 3A) and expert (Figure 3B).

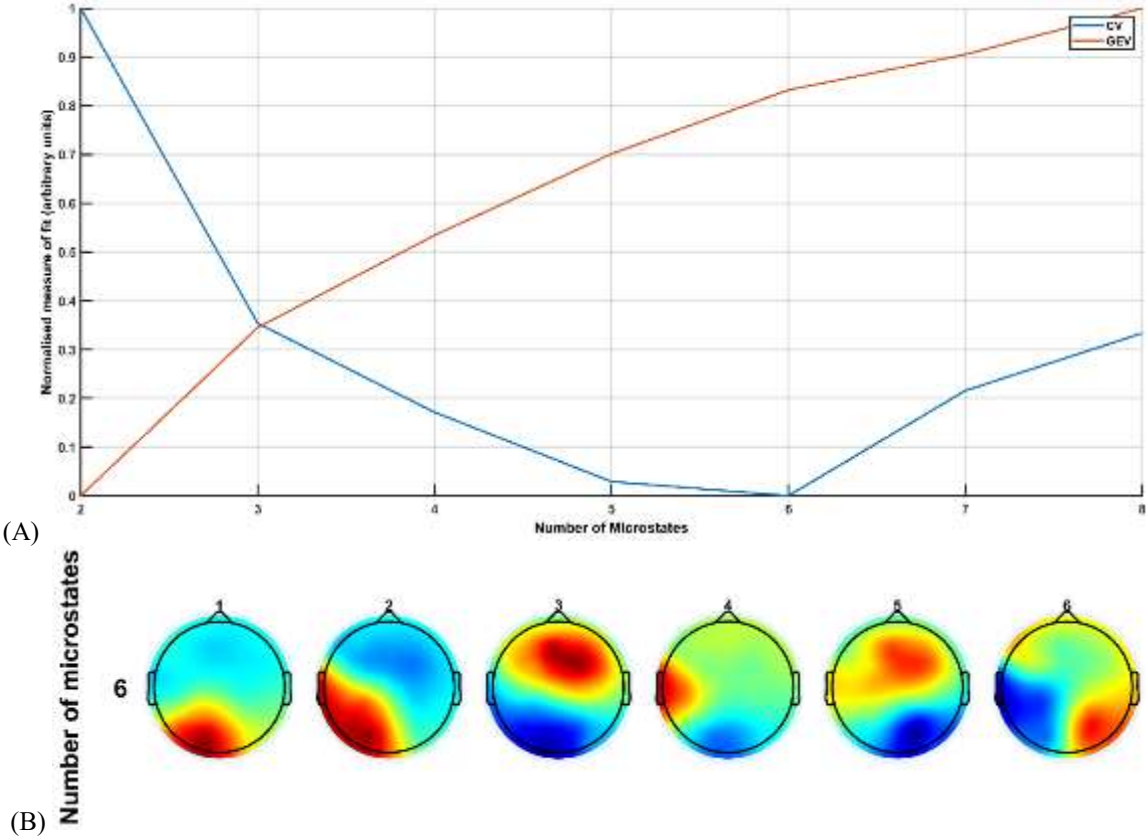

Figure 2: (A) Measures of fit plotted for the different microstate segmentation based on the global explained variance (GEV) and the cross-validation criterion (CV). (B) The selected six microstate prototypes based on the GEV and the CV criterion are sorted in decreasing GEV.

(A)

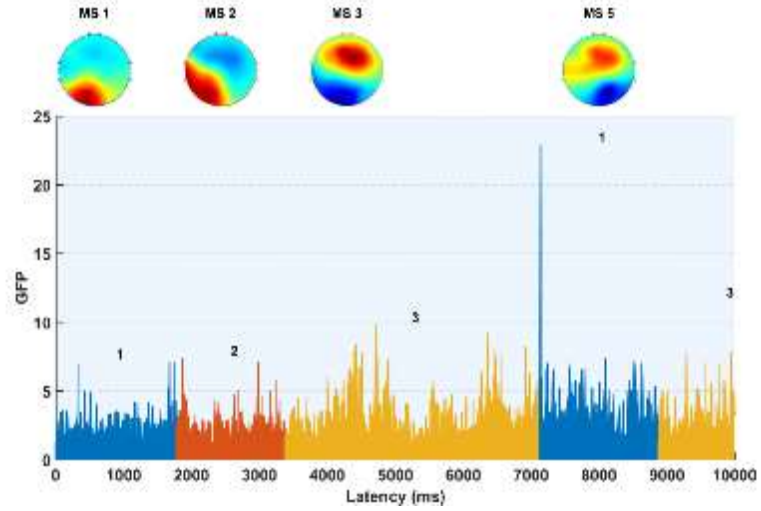

(B)

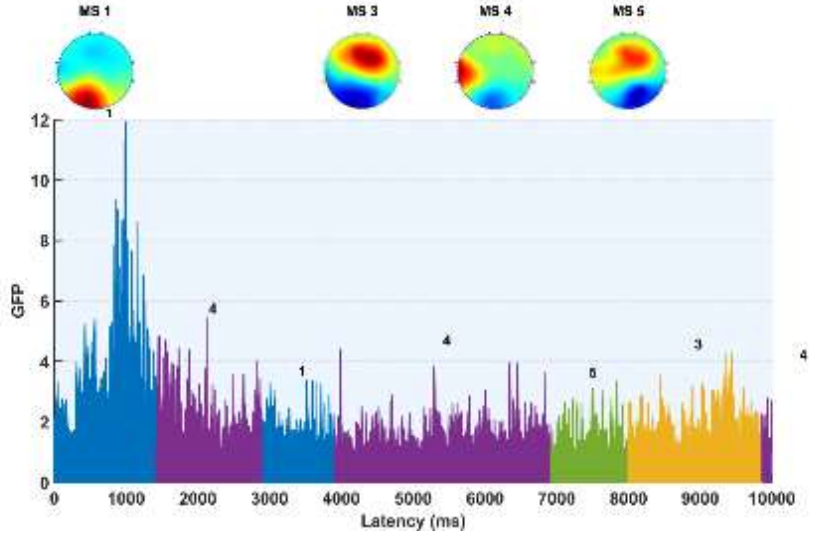

Figure 3: Illustrative figure of the GFP of active microstates, (A) during 0 to 10000 ms at the start of the FLS task of the EEG of a novice, (B) during 0 to 10000 ms at the start of the FLS task of the EEG of an expert.

The GFP of the active microstates at the start of the FLS task was subjected to CSP analysis to find the spatial filters. Then, after applying spatial filters to the expert's and novices' EEG data and extracting features from them, experts and novices were classified by LDA. We compared our microstate-based regularized CSP approach with conventional regularized CSP, where the microstate-based regularized CSP approach achieved a classification accuracy of 90.84% compared to 82.26% with the conventional regularized CSP. We also computed Kappa coefficient, which is a statistical method for measuring the degree of agreement between classes. Kappa coefficient method assigns zero to the random classification and one to the perfect classification (Townsend et al., 2006), which is a more robust criterion than classification accuracy by considering the random agreement. Microstate-based regularized CSP approach outperformed conventional regularized CSP with a Kappa coefficient of more than 0.9. Importantly, the microstate-based regularized CSP approach identified topographical maps from microstates 2 and 4 as the largest eigenvectors (from $M_2 = (C_1 + \alpha K)^{-1} C_2$ and $M_1 = (C_2 + \alpha K)^{-1} C_1$ respectively) so parietal hotspot was found to be important for discrimination (relevant for spatial binding (Zaretskaya et al., 2013) in the cognitive-perceptual model (Cioffi, 1991; Renner et al., 2013)).

Discussion

In the context of the perception-action cycle (Fuster, 2017), investigation of motor skill acquisition with various simulation technologies (Riener & Harders, 2012) can provide insights. Specifically, perception and action form a functional system through which the behavior is adapted in novice during motor learning to develop the perceptual memory initially. Perceptual memory in experts allows them to execute the task and reduce the variability in action to achieve perfection by updating the task parameters and refining them in the executive memory, a continuous process of exploitative learning. The two crucial attributes of the perception-action cycle are perceptual and executive memory (Fuster, 2004) which are subserved by the frontoparietal network (Marek & Dosenbach, 2018). In this study, microstate 2 was present in the illustrative novice (Figure 3A), while microstate 4 was present in the illustrative expert (Figure 3B) during the first 10 sec of the FLS task. It can be postulated that microstate four is associated with the activation of the left inferior parietal lobe (Numssen et al., 2021) since experts are expected to have the action semantics knowledge (van Elk, 2014). Also, a global Gestalt perception (Zaretskaya et al., 2013) is postulated to be present in the experts due to their experience. Then, the first 10 sec of FLS task-related brain states were captured in the illustrative expert and novice (Figure 3) also by the microstate 1 (corresponding to the activation of the visual cortex (Britz et al., 2010)), microstate 3 (corresponding to the attention reorientation (Britz et al., 2010) and medial frontal cortex activation (Gehring & Fencsik, 2001)), and the microstates 5 (topography comparable to microstate 3).

The scalp topography for the first spatial filter using our microstate-based regularized CSP approach identified topographical maps from microstates 2 and 4 as the most significant eigenvectors. Then, our microstate-based regularized CSP approach achieved classification accuracy greater than 90%. Here, microstate analysis applied a meta-criterion favoring the highest signal-to-noise ratio (Custo et al., 2017) that improved the accuracy when compared to that of conventional regularized CSP. Furthermore, microstates 2 and 4 as the most significant eigenvectors illustrated the importance of the EEG electrodes overlying the parietal cortex for the classification of experts and novices during the FLS task. Here, microstate 2 was dominant in the novices, while microstate 4 was dominant in the experts. While microstate 2 is comparable to right-frontal left-posterior microstate A of the prototypical microstate classes that account for most of the variance in resting-state EEG (Khanna et al., 2015), microstate 4 hotspot overlying temporoparietal junction and left inferior parietal lobe (Numssen et al., 2021) can be related to the intact perception of global gestalt (Rennig et al., 2013) which needs further investigation using EEG source localization. Also, Figure 3 illustrates the sequential flow of information between different brain states that can be related to perception-action coupling at the start of the FLS task, where EEG microstate sequences are known to be non-Markovian and nonstationary (Sikka et al., 2020). Here, recurrent neural networks can learn the underlying temporal dynamics and provide latent representations that can be sensitive to factors such as stress (Sikka et al., 2020). Therefore, studies need to investigate the temporal dynamics of microstates that the CSP approach could not capture in this study.

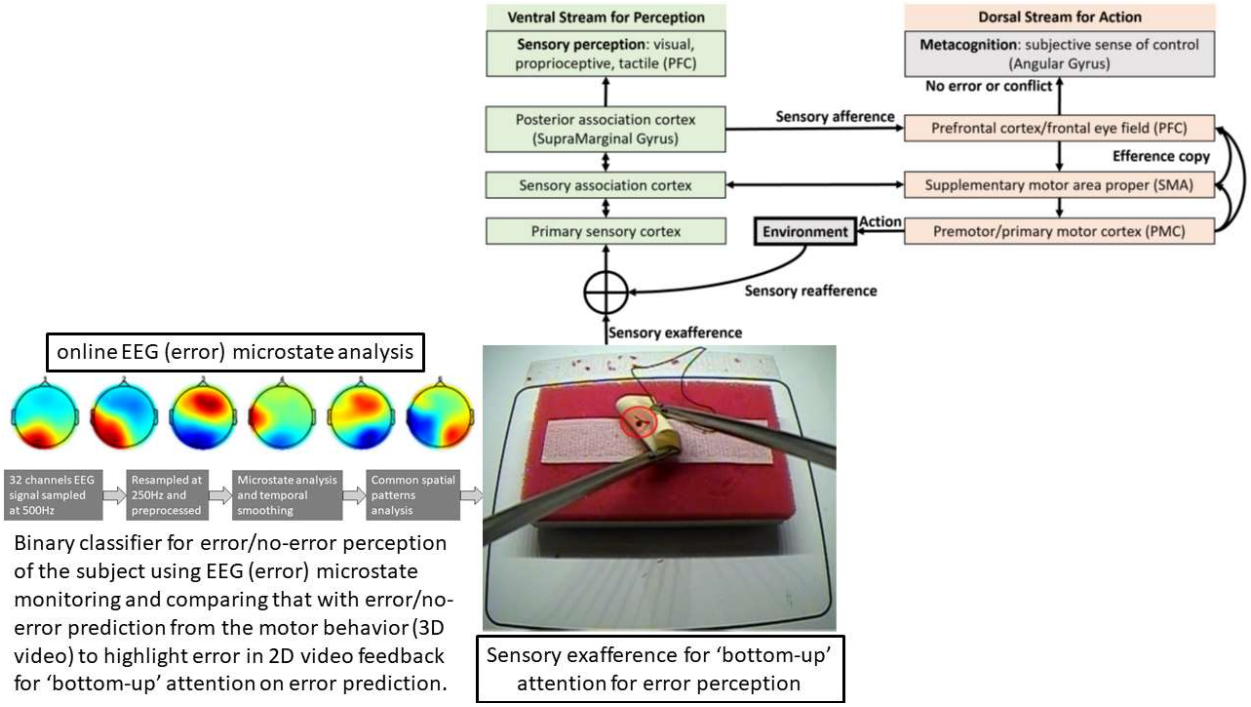

Figure 4: An adaptive VR-based training paradigm to facilitate error perception by highlighting the error in the 2D video feedback when the error perception is lacking in the subject.

A process for achieving interface and environment fidelity has been developed for the development of the Virtual Basic Laparoscopic Surgical Trainer (VBLaST) (Chellali et al., 2016). Then, Dutta et al. (Dutta et al., 2021) showed the importance of the brain-behavior relationship for investigating the neuroergonomics of the physical and virtual simulators that are crucial for validating Virtual Reality (VR) technology (Kamat et al., 2022). Then, monitoring the temporal dynamics of the brain-behavior can also allow an adaptive VR-based training paradigm (Zahabi & Abdul Razak, 2020), for example, for operant conditioning that has been shown feasible in our prior application for stroke rehabilitation (Kumar et al., 2019). Here, the VR training can be adapted based on the user's capabilities, performance, and needs (Zahabi & Abdul Razak, 2020) identified from brain-behavior monitoring. Microstate topographies can be used as a marker of proficiency such that the FLS psychomotor tasks with increasing task complexity can be progressed in the simulator as the novice trainee achieves proficiency towards FLS certification that uses all the five psychomotor tasks. For example, microstate 4 was associated with the activation of the left inferior parietal lobe (Numssen et al., 2021) related to the expert skill level (van Elk, 2014). In this study, the novice trainee attempted the most complex FLS suturing with an intracorporal knot tying task, so they had to start with building the perceptual model for task performance in the 3D environment based on 2D video feedback that is error prone (Tanagho et al., 2012). Figure 4 shows an application of online EEG microstate (brain) monitoring of subject-specific error perception that can be compared with the error prediction from the 3D (behavior) video data (from FLS box trainer) to facilitate subject's error perception by highlighting the error in 2D video feedback. Then, adjuvant treatment with portable neuroimaging guided non-invasive brain stimulation may be feasible to facilitate error-based learning (Walia et al., 2021).

In our prior work (Walia et al., 2021) on evaluating the feasibility of portable neuroimaging during the FLS task, we found that the average cortical activation in novices was primarily at the left pars opercularis of the inferior frontal gyrus involved in cognitive control (Levy & Wagner, 2011). Published studies have shown that the inferior frontal gyrus and the pre-supplementary motor area (pre-SMA) are involved in stop-signal task performance (Seidler et al., 2013) that is relevant in quick error correction. Then, the frontopolar prefrontal area (Walia et al., 2021) was more active in the experts, which may be related to the manipulation of (learned) structured information (Kroger & Kim, 2022). Specifically, neuroimaging of the rostrocaudal features of the frontal lobes that are associated with the varying degree of information processing complexity (Thiebaut de Schotten et al., 2017) may be relevant in driving closed-loop adaptive VR such that the task difficulty can be individualized to avoid stress response (also can be monitored with neuroimaging (Sikka et al., 2020)). Then, the supplementary motor area complex (SMA) is postulated to play the central role in descending from the prefrontal to the motor cortex for skill-related information flow. Here, SMA is involved in planning complex motor finger tasks (PE et al., 1980), considered the programming area for motor effector subroutines in bimanual coordination tasks. SMA has been suggested to form a queue of time-ordered motor commands before voluntary movement is executed via the descending pathways from the primary motor cortex (M1). In this study, microstate 5 is postulated to capture the SMA-related brain activity, which was more frequent in the experts than novices.

ACKNOWLEDGEMENTS

The authors gratefully acknowledge the support of this work through the Medical Technology Enterprise Consortium (MTEC) award #W81XWH2090019 (2020-628), and the US Army Futures Command, Combat Capabilities Development Command Soldier Center STTC cooperative research agreement #W912CG-21-2-0001.

CONFLICT STATEMENT

All authors declare that they have no conflicts of interest.

REFERENCES

Birkmeyer, J. D., Finks, J. F., O'Reilly, A., Oerline, M., Carlin, A. M., Nunn, A. R., Dimick, J., Banerjee, M., & Birkmeyer, N. J. O. (2013). Surgical Skill and Complication Rates after Bariatric Surgery. *New England Journal of Medicine*, *369*(15), 1434–1442. https://doi.org/10.1056/nejmsa1300625

Britz, J., Van De Ville, D., & Michel, C. M. (2010). BOLD correlates of EEG topography reveal rapid resting-state network dynamics. *NeuroImage*, *52*(4), 1162–1170. https://doi.org/10.1016/j.neuroimage.2010.02.052

Chang, C.-Y., Hsu, S.-H., Pion-Tonachini, L., & Jung, T.-P. (2020). Evaluation of Artifact Subspace Reconstruction for Automatic Artifact Components Removal in Multi-Channel EEG Recordings. *IEEE Transactions on Biomedical Engineering*, *67*(4), 1114–1121. https://doi.org/10.1109/TBME.2019.2930186

Chellali, A., Mentis, H., Miller, A., Ahn, W., Arikatla, V. S., Sankaranarayanan, G., De, S., Schwaitzberg, S. D., & Cao, C. G. L. (2016). Achieving interface and environment fidelity in the Virtual Basic Laparoscopic Surgical Trainer. *International Journal of Human-Computer Studies*, *96*, 22–37. https://doi.org/10.1016/j.ijhcs.2016.07.005

Christensen, A., Giese, M. A., Sultan, F., Mueller, O. M., Goericke, S. L., Ilg, W., & Timmann, D. (2014). An intact action-perception coupling depends on the integrity of the cerebellum. *The Journal of Neuroscience: The Official Journal of the Society for Neuroscience*, *34*(19), 6707–6716. https://doi.org/10.1523/JNEUROSCI.3276-13.2014

Cioffi, D. (1991). Beyond attentional strategies: Cognitive-perceptual model of somatic interpretation. *Psychological Bulletin*, *109*(1), 25–41. https://doi.org/10.1037/0033-2909.109.1.25

Crick, F. (1984). Function of the thalamic reticular complex: The searchlight hypothesis. *Proceedings of the National Academy of Sciences of the United States of America*, *81*(14), 4586–4590. https://doi.org/10.1073/pnas.81.14.4586

Custo, A., Van De Ville, D., Wells, W. M., Tomescu, M. I., Brunet, D., & Michel, C. M. (2017). Electroencephalographic Resting-State Networks: Source Localization of Microstates. *Brain Connectivity*, *7*(10), 671–682. https://doi.org/10.1089/brain.2016.0476

Dehabadi, M., Fernando, B., & Berlingieri, P. (2014). The use of simulation in the acquisition of laparoscopic suturing skills. *International Journal of Surgery*, *12*(4), 258–268. https://doi.org/10.1016/J.IJSU.2014.01.022

Dutta, A., Kamat, A., Makled, B., Norfleet, J., Intes, X., & De, S. (2021). Interhemispheric Functional Connectivity in the Primary Motor Cortex Distinguishes Between Training on a Physical and a Virtual Surgical Simulator. In M. de Bruijne, P. C. Cattin, S. Cotin, N. Padoy, S. Speidel, Y. Zheng, & C. Essert (Eds.), *Medical Image Computing and Computer Assisted Intervention – MICCAI 2021* (pp. 636–644). Springer International Publishing. https://doi.org/10.1007/978-3-030-87202-1_61

Ericsson, K. A., & Harwell, K. W. (2019). Deliberate Practice and Proposed Limits on the Effects of Practice on the Acquisition of Expert Performance: Why the Original Definition Matters and Recommendations for Future Research. *Frontiers in Psychology*, *10*. https://www.frontiersin.org/article/10.3389/fpsyg.2019.02396

Fuster, J. M. (2004). Upper processing stages of the perception-action cycle. *Trends in Cognitive Sciences*, *8*(4), 143–145. https://doi.org/10.1016/j.tics.2004.02.004

Fuster, J. M. (2017). Chapter 8 - Prefrontal Cortex in Decision-Making: The Perception–Action Cycle. In J.-C. Dreher & L. Tremblay (Eds.), *Decision Neuroscience* (pp. 95–105). Academic Press. https://doi.org/10.1016/B978-0-12-805308-9.00008-7

Gehring, W. J., & Fencsik, D. E. (2001). Functions of the Medial Frontal Cortex in the Processing of Conflict and Errors. *The Journal of Neuroscience*, *21*(23), 9430–9437. https://doi.org/10.1523/JNEUROSCI.21-23-09430.2001

Gu, Q. L., Lam, N. H., Wimmer, R. D., Halassa, M. M., & Murray, J. D. (2021). *Computational Circuit Mechanisms Underlying Thalamic Control of Attention* (p. 2020.09.16.300749). https://doi.org/10.1101/2020.09.16.300749

Hughes, S. W., Lörincz, M., Cope, D. W., Blethyn, K. L., Kékesi, K. A., Parri, H. R., Juhász, G., & Crunelli, V. (2004). Synchronized Oscillations at α and θ Frequencies in the Lateral Geniculate Nucleus. *Neuron*, *42*(2), 253–268. https://doi.org/10.1016/S0896-6273(04)00191-6

Hurley, S. (2001). Perception and Action: Alternative Views. *Synthese*, *129*(1), 3–40.

Kamat, A., Makled, B., Norfleet, J., Schwaitzberg, S. D., Intes, X., De, S., & Dutta, A. (2022). Directed information flow during laparoscopic surgical skill acquisition dissociated skill level and medical simulation technology. *Npj Science of Learning*, *7*(1), 1–13. https://doi.org/10.1038/s41539-022-00138-7

Kawato, M. (1999). Internal models for motor control and trajectory planning. *Current Opinion in Neurobiology*, *9*(6), 718–727. https://doi.org/10.1016/s0959-4388(99)00028-8

Khanna, A., Pascual-Leone, A., Michel, C. M., & Farzan, F. (2015). Microstates in resting-state EEG: Current status and future directions. *Neuroscience and Biobehavioral Reviews*, *49*, 105–113. https://doi.org/10.1016/j.neubiorev.2014.12.010

Koles, Z. J. (1991). The quantitative extraction and topographic mapping of the abnormal components in the clinical EEG. *Electroencephalography and Clinical Neurophysiology*, *79*(6), 440–447. https://doi.org/10.1016/0013-4694(91)90163-X

Kothe, C. A., & Makeig, S. (2013). BCILAB: A platform for brain-computer interface development. *Journal of Neural Engineering*, *10*(5), 056014. https://doi.org/10.1088/1741-2560/10/5/056014

Kroger, J., & Kim, C. (2022). Frontopolar Cortex Specializes for Manipulation of Structured Information. *Frontiers in Systems Neuroscience*, *16*. https://www.frontiersin.org/article/10.3389/fnsys.2022.788395

Kumar, D., Sinha, N., Dutta, A., & Lahiri, U. (2019). Virtual reality-based balance training system augmented with operant conditioning paradigm. *BioMedical Engineering OnLine*, *18*(1), 90. https://doi.org/10.1186/s12938-019-0709-3

Levy, B. J., & Wagner, A. D. (2011). Cognitive control and right ventrolateral prefrontal cortex: Reflexive reorienting, motor inhibition, and action updating. *Annals of the New York Academy of Sciences*, *1224*(1), 40–62. https://doi.org/10.1111/j.1749-6632.2011.05958.x

Lotte, F., & Guan, C. (2011). Regularizing Common Spatial Patterns to Improve BCI Designs: Unified Theory and New Algorithms. *IEEE Transactions on Biomedical Engineering*, *58*(2), 355–362. https://doi.org/10.1109/TBME.2010.2082539

Lu, H., Eng, H.-L., Guan, C., Plataniotis, K. N., & Venetsanopoulos, A. N. (2010). Regularized Common Spatial Pattern With Aggregation for EEG Classification in Small-Sample Setting. *IEEE Transactions on Biomedical Engineering*, *57*(12), 2936–2946. https://doi.org/10.1109/TBME.2010.2082540

Marek, S., & Dosenbach, N. U. F. (2018). The frontoparietal network: Function, electrophysiology, and importance of individual precision mapping. *Dialogues in Clinical Neuroscience*, *20*(2), 133–140.

Marucci, M., Di Flumeri, G., Borghini, G., Sciaraffa, N., Scandola, M., Pavone, E. F., Babiloni, F., Betti, V., & Aricò, P. (2021). The impact of multisensory integration and perceptual load in virtual reality settings on performance, workload and presence. *Scientific Reports*, *11*(1), 4831. https://doi.org/10.1038/s41598-021-84196-8

Michel, C. M., & Koenig, T. (2018). EEG microstates as a tool for studying the temporal dynamics of whole-brain neuronal networks: A review. *NeuroImage*, *180*, 577–593. https://doi.org/10.1016/j.neuroimage.2017.11.062

Numssen, O., Bzdok, D., & Hartwigsen, G. (2021). Functional specialization within the inferior parietal lobes across cognitive domains. *ELife*, *10*, e63591. https://doi.org/10.7554/eLife.63591

PE, R., B, L., NA, L., & E, S. (1980). Supplementary motor area and other cortical areas in organization of voluntary movements in man. *Journal of Neurophysiology*, *43*(1), 118–136. https://doi.org/10.1152/JN.1980.43.1.118

Perrin, F., Pernier, J., Bertrand, O., & Echallier, J. F. (1989). Spherical splines for scalp potential and current density mapping. *Electroencephalography and Clinical Neurophysiology*, *72*(2), 184–187. https://doi.org/10.1016/0013-4694(89)90180-6

Poldrack, R. A., Sabb, F. W., Foerde, K., Tom, S. M., Asarnow, R. F., Bookheimer, S. Y., & Knowlton, B. J. (2005). The Neural Correlates of Motor Skill Automaticity. *The Journal of Neuroscience*, *25*(22), 5356–5364. https://doi.org/10.1523/JNEUROSCI.3880-04.2005

Poulsen, A. T., Pedroni, A., Langer, N., & Hansen, L. K. (2018). *Microstate EEGlab toolbox: An introductory guide*. https://doi.org/10.1101/289850

Renner, R. S., Velichkovsky, B. M., & Helmert, J. R. (2013). The perception of egocentric distances in virtual environments—A review. *ACM Computing Surveys*, *46*(2), 23:1-23:40. https://doi.org/10.1145/2543581.2543590

Rennig, J., Bilalic, M., Huberle, E., Karnath, H.-O., & Himmelbach, M. (2013). The temporo-parietal junction contributes to global gestalt perception—Evidence from studies in chess experts. *Frontiers in Human Neuroscience*, *7*. https://www.frontiersin.org/article/10.3389/fnhum.2013.00513

Riener, R., & Harders, M. (2012). *Virtual Reality in Medicine*. Springer-Verlag. https://doi.org/10.1007/978-1-4471-4011-5

Seidler, R. D., Kwak, Y., Fling, B. W., & Bernard, J. A. (2013). Neurocognitive Mechanisms of Error-Based Motor Learning. *Advances in Experimental Medicine and Biology*, *782*, 10.1007/978-1-4614-5465-6_3. https://doi.org/10.1007/978-1-4614-5465-6_3

Sikka, A., Jamalabadi, H., Krylova, M., Alizadeh, S., van der Meer, J. N., Danyeli, L., Deliano, M., Vicheva, P., Hahn, T., Koenig, T., Bathula, D. R., & Walter, M. (2020). Investigating the temporal dynamics of electroencephalogram (EEG) microstates using recurrent neural networks. *Human Brain Mapping*, *41*(9), 2334–2346. https://doi.org/10.1002/hbm.24949

Sommer, M. A., & Wurtz, R. H. (2008). Brain circuits for the internal monitoring of movements. *Annual Review of Neuroscience*, *31*, 317–338. https://doi.org/10.1146/annurev.neuro.31.060407.125627

Tamber-Rosenau, B. J., Esterman, M., Chiu, Y.-C., & Yantis, S. (2011). Cortical Mechanisms of Cognitive Control for Shifting Attention in Vision and Working Memory. *Journal of Cognitive Neuroscience*, *23*(10), 2905–2919. https://doi.org/10.1162/jocn.2011.21608

Tanagho, Y. S., Andriole, G. L., Paradis, A. G., Madison, K. M., Sandhu, G. S., Varela, J. E., & Benway, B. M. (2012). 2D versus 3D visualization: Impact on laparoscopic proficiency using the fundamentals of laparoscopic surgery skill set. *Journal of Laparoendoscopic & Advanced Surgical Techniques. Part A*, *22*(9), 865–870. https://doi.org/10.1089/lap.2012.0220

Thiebaut de Schotten, M., Urbanski, M., Batrancourt, B., Levy, R., Dubois, B., Cerliani, L., & Volle, E. (2017). Rostro-caudal Architecture of the Frontal Lobes in Humans. *Cerebral Cortex (New York, N.Y.: 1991)*, *27*(8), 4033–4047. https://doi.org/10.1093/cercor/bhw215

Townsend, G., Graimann, B., & Pfurtscheller, G. (2006). A comparison of common spatial patterns with complex band power features in a four-class BCI experiment. *IEEE Transactions on Biomedical Engineering*, *53*(4), 642–651. https://doi.org/10.1109/TBME.2006.870237

van Elk, M. (2014). The left inferior parietal lobe represents stored hand-postures for object use and action prediction. *Frontiers in Psychology*, *5*. https://www.frontiersin.org/article/10.3389/fpsyg.2014.00333

Voorhorst, F., Meijer, D., Overbeeke, C., & Smets, G. (1998). Depth perception in laparoscopy through perception-action coupling. *Minimally Invasive Therapy & Allied Technologies*, *7*(4), 325–334. https://doi.org/10.3109/13645709809152876

Walia, P., Fu, Y., Schwaitzberg, S. D., Intes, X., De, S., Cavuoto, L., & Dutta, A. (2021). *Neuroimaging guided tES to facilitate complex laparoscopic surgical tasks – insights from functional near-infrared spectroscopy*. https://doi.org/10.21203/rs.3.rs-730076/v1

Wolpert, D. M., & Miall, R. C. (1996). Forward Models for Physiological Motor Control. *Neural Networks: The Official Journal of the International Neural Network Society*, *9*(8), 1265–1279. https://doi.org/10.1016/s0893-6080(96)00035-4

Zahabi, M., & Abdul Razak, A. M. (2020). Adaptive virtual reality-based training: A systematic literature review and framework. *Virtual Reality*, *24*(4), 725–752. https://doi.org/10.1007/s10055-020-00434-w

Zaretskaya, N., Anstis, S., & Bartels, A. (2013). Parietal Cortex Mediates Conscious Perception of Illusory Gestalt. *Journal of Neuroscience*, *33*(2), 523–531. https://doi.org/10.1523/JNEUROSCI.2905-12.2013